CRISPR BIOLOGY

A cyclic oligonucleotide signaling pathway in type III CRISPR-Cas systems

Migle Kazlauskiene, Georgij Kostiuk, Česlovas Venclovas, Gintautas Tamulaitis,* Virginijus Siksnys*

Type III CRISPR-Cas systems in prokaryotes provide immunity against invading nucleic acids through the coordinated degradation of transcriptionally active DNA and its transcripts by the Csm effector complex. The Cas10 subunit of the complex contains an HD nuclease domain that is responsible for DNA degradation and two Palm domains with elusive functions. In addition, Csm6, a ribonuclease that is not part of the complex, is also required to provide full immunity. We show here that target RNA binding by the Csm effector complex of *Streptococcus thermophilus* triggers Cas10 to synthesize cyclic oligoadenylates (cA_n; n = 2 to 6) by means of the Palm domains. Acting as signaling molecules, cyclic oligoadenylates bind Csm6 to activate its nonspecific RNA degradation. This cyclic oligoadenylate–based signaling pathway coordinates different components of CRISPR-Cas to prevent phage infection and propagation.

In the prokaryotic type III CRISPR-Cas (clustered regularly interspaced short palindromic repeats and CRISPR-associated genes) systems, multiple Cas proteins assemble with CRISPR RNA (crRNA) into Csm (type III-A) (Fig. 1A) or Cmr (type III-B) effector complexes that provide interference against invading nucleic acids through transcription-dependent DNA silencing (*1*). After infection, the transcription of phage DNA is initiated to establish and maintain the infection cycle. In bacteria, the crRNA-guided Csm/Cmr complex acts as a surveillance complex that scans for the complementary target sequence (a protospacer) in the invader's RNA. Tethering of the Csm/Cmr complex to the transcript by crRNA triggers RNA cleavage by Csm3/Cmr4 subunits and simultaneously activates the single-stranded deoxyribonuclease (ssDNase) activity of the Cas10 subunit for coupled degradation of the ssDNA in the transcription bubble. Csm/Cmr complexes avoid autoimmunity by checking the complementarity between the crRNA 5′-handle, which originates from the CRISPR repeat, and the 3′-sequence flanking the target sequence in RNA. Base-pairing between the crRNA 5′-handle and the target RNA represses the Cas10 ssDNase activity, thus protecting the host DNA from degradation. Noncomplementarity of the crRNA 5′-handle to the RNA target in the phage RNA specifies a nonself DNA template and activates the Cas10 ssDNase (*2*–*4*).

The Cas10 subunit (called Csm1 and Cmr2 in the type III-A and III-B systems, respectively) harbors an N-terminal HD domain, two small α-helical domains, and two Palm domains that share a ferredoxin-like fold with the core domain of nucleic acid polymerases and nucleotide cyclases (*5*–*7*). The HD domain of Cas10 is responsible for ssDNA degradation in vitro. The conserved GGDD motif in one of the two Palm domains has been hypothesized to generate cyclic nucleotides (*8*), but its role remains to be established (*1*, *3*, *4*, *9*, *10*). The crystal structures of *Pyroccocus furiosus* Cas10 (PfCas10) alone and the PfCas10-Cmr3 subcomplex show a single adenosine diphosphate (ADP), a single adenosine 3′-monophosphate (3′-AMP), or two adenosine triphosphate (ATP) molecules bound by amino acid residues of the GGDD and P-loop motifs in the Palm domains (*5*, *7*, *11*). The conservation of the adenine binding pocket and catalytic residues typical of Palm domain polymerases and cyclases provided a hint that the Palm domain of Cas10 might be enzymatically active, but the nature of this activity has remained unknown. This prompted us to investigate a possible ATP-dependent catalytic activity of *S. thermophilus* DGCC8004 Cas10 (StCas10) from a type III-A CRISPR-Cas system.

StCas10 alone, or in the context of the StCsm binary complex [$Cas10_1$:$Csm2_3$:$Csm3_5$:$Csm4_1$:$Csm5_1$:$crRNA_1$, 40 nucleotides (nt)], shows no activity toward ATP (fig. S1, A to C). However, the StCsm ternary complex with target RNA converts ATP into product X, which migrates faster than ATP but slower than ADP in thin-layer chromatography (Fig. 1B and fig. S1, D and E). Notably, only target RNA S3/2, which is complementary to the crRNA spacer, but not to the crRNA 5′-handle, stimulates ATP conversion to product X (Fig. 1B). Thus, the noncomplementarity of the crRNA 5′-handle to the 3′-flanking sequence of target RNA (Fig. 1B and fig. S2) controls the ATP reaction, similar to the ssDNase activity of the HD domain. Furthermore, target RNA binding, but not cleavage, is required to initiate this reaction (fig. S3). Importantly, the D16A mutation that compromises ssDNase activity has no effect on the ATP reaction, whereas the double D575A+D576A mutation in the GGDD motif of the Cas10 Palm domain abrogates ATP conversion into product X (Fig. 1C and fig. S4). This reaction is dependent on Mn^{2+}, Co^{2+}, or Zn^{2+} and to a lesser degree on Mg^{2+} or Fe^{2+} (fig. S5). Taken together, these data demonstrate that the GGDD motif of the Cas10 subunit in StCsm is responsible for a metal-dependent ATP conversion into a reaction product X, and this reaction is critically dependent on the target RNA recognition and the noncomplementarity of the crRNA 5′-handle to the 3′-flanking sequence of target RNA.

Both binary and ternary StCsm complexes bind ATP tightly (dissociation constant $K_d \approx 20$ nM), but not uridine triphosphate (UTP) or cytidine triphosphate (CTP). Binary StCsm also shows low affinity toward guanosine triphosphate (GTP) (fig. S6). The D575A+D576A mutation in the Cas10 GGDD motif disrupts ATP binding (fig. S4C), implying that ATP is bound by the Palm domain. The ternary StCsm complex binds 2′dATP with much lower affinity (by a factor of ~15) than ATP or 3′dATP. No reaction products are formed in the 3′dATP, UTP, GTP, CTP, AMP, and ADP reactions, but StCsm still exhibits low activity on 2′dATP (fig. S7). Moreover, AMP cross-reacts with ATP, 2′dATP, and 3′dATP to produce respective dinucleotides (fig. S8). This finding implies that Cas10 has at least two adenosine binding sites that may accommodate different nucleotides, in agreement with the crystal structures of PfCas10 (*11*). In AMP cross-reactions, one pocket presumably accommodates AMP while another binds ATP, 2′dATP, or 3′dATP. These experiments together reveal minimal substrate requirements for the reactions catalyzed by the StCas10 Palm domain: (i) It must contain adenine, (ii) at least one nucleotide partner must contain 3′-OH in a ribose, and (iii) the triphosphate moiety is necessary in another partner for the reaction to occur.

Next, we aimed to identify the StCsm-mediated reaction product X. Polyacrylamide gel electrophoresis under denaturing conditions revealed several bands, with the major one migrating similarly to linear hexa-adenylate (A_6) (Fig. 2A). High-performance liquid chromatography–mass spectrometry (HPLC-MS) analysis revealed that the predominant reaction product (63.6%) had a molecular mass of 987.15 Da (Fig. 2B). Such a mass could correspond to either cyclic tri-adenylate (cA_3) or linear A_3 containing terminal 2′,3′-cyclic phosphate (A_3>p) (fig. S9). Reaction products with masses corresponding to the analogous tetra- (17.7%), penta- (8.0%), hexa- (0.5%), and di-adenylates, as well as linear pA_3, ppA_3, pA_2, and $pppA_2$ (10.2%, collectively) (fig. S9), were also detected in the ATP reaction.

We next used HPLC to purify oligoadenylates (OAs) (fig. S10) and probed their chemical structure by means of biochemical assays. Although the major reaction product was resistant to the PDE12 nuclease (Fig. 2A and fig. S11), which exhibits exonuclease activity on linear 2′,5′- and 3′,5′-OAs (*12*), the P1 endonuclease degraded it to AMP (Fig. 2A and fig. S12). MS analysis confirmed that neither adenosine nor adenosine 2′,3′-cyclic phosphate, which would result from the P1 nuclease-mediated hydrolysis of A_3>p, were produced (Fig. 2C and fig. S12). Other OAs synthesized by StCsm were cleaved by P1 nuclease in the same manner (fig. S12), suggesting that they are cyclic. Moreover, these OAs could not be 5′-labeled by polynucleotide

Institute of Biotechnology, Vilnius University, Saulėtekio Avenue 7, 10257 Vilnius, Lithuania.
*Corresponding author. Email: tamulaitis@ibt.lt (G.T.); siksnys@ibt.lt (V.S.)

Downloaded from https://www.science.org at Shanghai Normal University on March 29, 2025

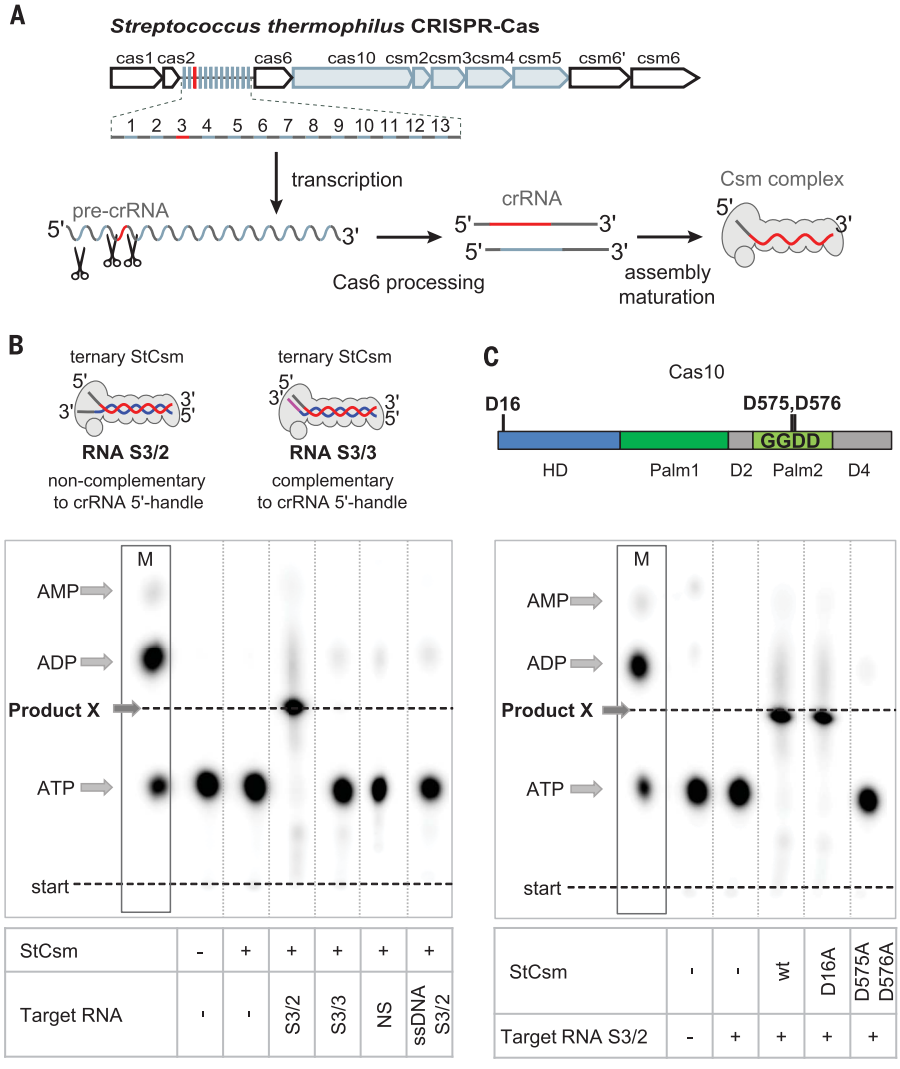


Fig. 1. StCsm complex–mediated conversion of ATP to the reaction products. (**A**) Schematic organization of the *S. thermophilus* type III-A CRISPR-Cas locus. Spacers interspaced between repeats are numbered. The transcribed CRISPR RNA is processed and bound by Cas proteins to form a *S. thermophilus* Csm (StCsm) complex. The mature crRNA guides the StCsm complex in the recognition of an invader transcript at the interference stage. (**B**) Target RNA sequence requirements for the StCsm-mediated conversion of ATP to the reaction products. Cartoons above the gels depict reaction components; the target sequence is blue, the complementary strand (matching spacer in crRNA) is red, and the 3′-flanking sequence of protospacer complementary to the 5′-handle of crRNA is pink. (**C**) Effect of mutations in StCsm Cas10 HD and Palm domains on the conversion of ATP to the reaction products. The domain architecture of the StCas10 protein is presented above the gels. HD denotes an HD-type phosphohydrolase/nuclease domain (blue); the two Palm domains are polymerase/cyclase–like Palm domains, one of which contains a GGDD motif (green); D2 and D4 denote α-helical domains (gray). Conserved active site residues subjected to alanine mutagenesis are indicated above the colored boxes. M, ATP partial thermal hydrolysis ladder; wt, wild type. Throughout, single-letter abbreviations for the amino acid residues are as follows: A, Ala; D, Asp; G, Gly; H, His; K, Lys; N, Asn; Q, Gln; R, Arg; S, Ser; T, Thr; X, any amino acid.

kinase (Fig. 2A and fig. S13), confirming the absence of a free terminal 5′-OH group, again consistent with the cyclic structure. Collectively, these data indicate that StCsm synthesizes a mixture of cyclic OAs (cOAs), with cA_3 being the predominant product.

Because the P1 nuclease, which exhibits high phosphomonoesterase activity toward 3′,5′- but not 2′,5′-ribonucleotides (*13*), effectively cleaves cA_3 to AMP, the cOA is likely to possess all three 3′-5′ phosphodiester bonds. Reactions with 2′dATP, 3′dATP, and AMP (figs. S7 and S8) showed that a 3′-OH, but not a 2′-OH, is required for the reaction. It seems likely that the cOA is generated by polymerization of ATP molecules into linear OA, followed by subsequent cyclization (Fig. 2D).

StCas10 contains two Palm domains, P and P*, both of which are capable of binding ATP, but only one of which features the conserved catalytic GGDD motif. ATP binding in the P site positions the 3′-OH for the nucleophilic attack on the αP atom of the ATP molecule bound in the P* site. Subsequent inter- and intramolecular nucleophilic reactions yield different cOAs (Fig. 2B). To confirm this reaction mechanism, we synthesized the linear OA triphosphates $pppA_3$ to $pppA_6$ and used them as substrates for the StCsm-catalyzed cyclization reaction. Upon treatment with wild-type ternary StCsm, these OA triphosphates were converted to corresponding cOAs (Fig. 2E and fig. S14). This proves that linear OA triphosphates act as intermediates in the StCsm-mediated ATP polymerization and cyclization reactions.

Taken together, these data demonstrate that the GGDD active site of Cas10 subunit in the StCsm complex catalyzes the synthesis of cOAs in response to the invasion of viral nucleic acid. Small nucleotide-based compounds such as cAMP, cyclic GMP-AMP (cGAMP), p_2Gpp, p_3Gpp, nicotinic acid adenine dinucleotide phosphate, cyclic adenosine diphosphoribose, and 2′,5′-OAs often act as signaling molecules in various organisms (*14*). Therefore, we hypothesized that the cOAs described here could also act as signaling molecules in an antiviral defense pathway in prokaryotes. Given that nucleotide-based messengers usually bind to sensory proteins that generate the response, we next aimed to identify a sensor for cOAs.

Many CRISPR-Cas systems are associated with genes that appear not to be directly implicated in spacer acquisition, CRISPR transcript processing, or interference against invading nucleic acids (*6*, *15*). Among them, the most common are the genes coding for Csm6/Csx1 proteins (*6*). The type III-A CRISPR-Cas locus in the *S. thermophilus* DGCC8004 strain encodes two Csm6 homologs (StCsm6 and StCsm6′), although neither is part of the StCsm surveillance complex (*16*). Both proteins have conserved Csm6 architecture: the N-terminal CARF (CRISPR-associated Rossman fold) domain, followed by the α-helical region (6H domain) and the C-terminal HEPN (higher eukaryotes and prokaryotes nucleotide-binding) domain (Fig. 3A) (*17*–*19*). Molecular modeling revealed that the core of the CARF domain in both StCsm6 and StCsm6′ is most similar to the corresponding domain in the *Thermus thermophilus* Csm6 structure [TtCsm6; Protein Data Bank (PDB) ID, 5FSH] (*17*) (fig. S15). The HEPN domain is more akin to that of *Streptococcus mutans* Csm6 (PDB ID, 4RGP) (fig. S16). Domains belonging to the HEPN superfamily often exhibit ribonuclease activity and are commonly found in prokaryotic toxin-antitoxin and abortive infection defense systems (*20*).

To understand the role of Csm6 proteins in *S. thermophilus* CRISPR-Cas immunity, we expressed His-tagged versions of StCsm6 (fig. S17B) and StCsm6′ (fig. S18B) in *Escherichia coli* and isolated them by affinity chromatography. Both StCsm6 and StCsm6′—like the homologous *Staphylococcus epidermidis* Csm6, TtCsm6, *Pyrococcus horikoshii* Csm6, and PfCsx1 proteins (*17*, *19*, *21*)—showed ssRNA degradation activity in a metal-independent

Downloaded from https://www.science.org at Shanghai Normal University on March 29, 2025

manner, reliant on conserved HEPN active site residues (RXXXXH) (figs. S17, D and F, and S18, D and E). Notably, their ssRNase activity was weak and evident only at high (micromolar range) protein concentrations (Fig. 3B and figs. S17D and S18D). We hypothesized that cOAs produced by the StCsm complex could act as ligands for the CARF domain of StCsm6 and/or StCsm6′. The mixture of cOAs dramatically increased the ssRNase activity of both StCsm6 and StCsm6′, reducing the required protein concentration by a factor of ~1000 (Fig. 3B and figs. S17D and S18D). Both dsRNA and ssDNA were resistant to hydrolysis in both the absence and presence of cOAs (fig. S19), confirming that StCsm6 and StCsm6′ are ssRNA-specific nucleases.

StCsm6 and StCsm6′, like TtCsm6, are homodimers in solution (figs. S17C and S18C) (*17*). Also like TtCsm6, both StCsm6 and StCsm6′ feature a putative ligand binding site at the dimer interface of the CARF domains (Fig. 3A). On the basis of docking experiments and surface conservation, we identified residues that may be involved in ligand binding in TtCsm6, StCsm6, and StCsm6′. Mutations of the StCsm6 putative ligand-binding residues H24, N102, S105, T107, or Q129 significantly decreased the StCsm6 ssRNase activity induced by cOAs, indicating that the cOA binding to the CARF domain allosterically regulates the ssRNase activity of the HEPN domain (Fig. 3C and fig. S17E). Collectively, these data reveal that the CARF domain of Csm6 proteins acts as a sensor for the cOA ligand produced by the StCsm complex. Importantly, although biologically relevant ATP concentrations inhibit the StCsm6 RNase, it can be easily rescued by cOAs (fig. S20).

Next, we aimed to determine which of the cOAs synthesized by the ternary StCsm complex is the activator of StCsm6 and StCsm6′. Nuclease assays revealed that of all the cOAs tested (cA_n, n = 2 to 6), only cA_6 stimulated ribonuclease activity of StCsm6/StCsm6′ (Fig. 3D and fig. S21). Although only low amounts of cA_6 were synthesized by StCsm in vitro, it cannot be excluded that the reaction equilibrium is shifted to longer cOAs in vivo. Nevertheless, 0.5 nM cA_6 was sufficient to trigger robust StCsm6 ribonuclease activity, although 5 nM cA_6 was necessary in the case of StCsm6′. The StCsm6- and Csm6′-mediated RNA cleavage occurred preferentially at GA or AA dinucleotides, although the addition of cA_6 broadened the cleavage preference (fig. S22). The StCsm6 and StCsm6′ proteins show 34% amino acid identity. StCsm6′ could have evolved in response to the inhibiting phage factors, such as anti-CRISPR (*22*), that targeted the Csm6 ribonuclease. Intriguingly, cA_4, but not cA_6, stimulated TtCsm6 ribonuclease activity (Fig. 3E and fig. S23). This is consistent with docking and structure modeling experiments that suggest four possible adenosine binding sites in the dimeric TtCsm6 CARF domain structure (fig. S15D). Under the same reaction conditions, linear OAs did not activate StCsm6 or TtCsm6 (fig. S24). Seemingly, the cOAs are universal signaling molecules in various type III CRISPR-Cas systems, although the size of the signaling molecule may be specific for a given system. This finding implies that Csm6/Csx1 and other CARF family proteins associated with Csm/Cmr complexes (*17*–*19*, *23*–*25*) may be regulated by cOAs. Interestingly, target RNA binding by the Cas13a protein of the type VI-A CRISPR-Cas system triggers degradation of collateral ssRNA, which has no complementarity to the crRNA, in the absence of any signaling molecules (*26*).

Cyclic dinucleotides (c-di-GMP, c-di-AMP, or cGAMP) are often encountered across the three

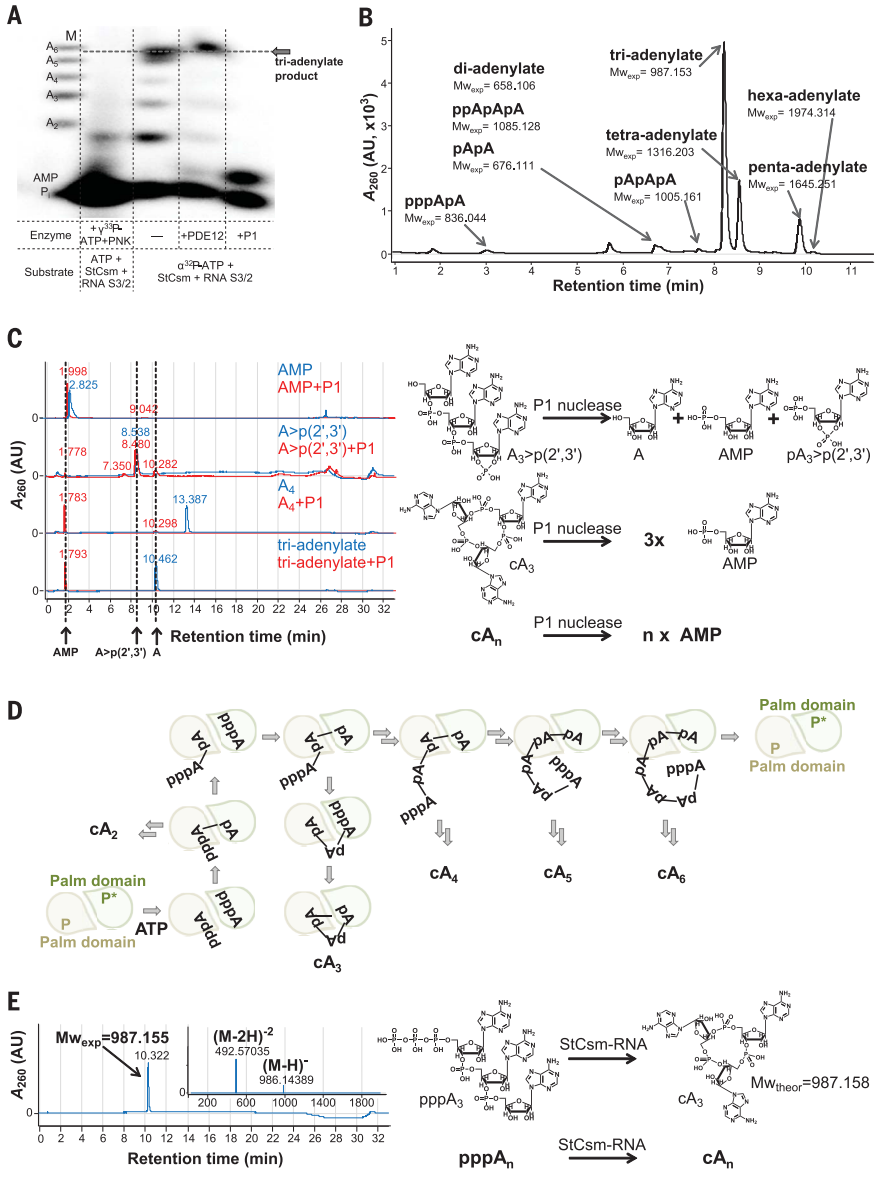


Fig. 2. Identification of the StCsm-mediated ATP reaction products. (**A**) Treatment of ATP reaction products with T4 polynucleotide kinase and PDE12 or P1 nuclease. The tri-adenylate product (gray arrow) migrates differently from linear A_3, indicative of its nonlinear structure. P_i, (pyro)phosphate; PNK, T4 polynucleotide kinase. (**B**) Characterization of ATP reaction products by electrospray ionization–MS analysis. Identified masses (Mw_{exp}, in daltons) and compounds are presented above the HPLC chromatogram. A_{260}, absorbance at 260 nm; AU, arbitrary units. (**C**) HPLC-MS analysis of the tri-adenylate digest by P1 nuclease (left) and scheme for P1-mediated cA_3 or linear A_3 hydrolysis (right). (**D**) Proposed model for the StCsm-mediated ATP polymerase/cyclase reaction mechanism. Both StCas10 Palm domains (P and P*) can bind ATP, but only one features the conserved GGDD motif and is catalytically active. ATP binding in the P site positions the 3′-OH for nucleophilic attack on α-phosphorous of ATP bound in the P* site to produce $pppA_2$. $pppA_2$ can then rearrange between P and P*, positioning the 3′-OH group for internal nucleophilic attack on its own triphosphate moiety to yield cA_2 or translocate between the sites to react with a new ATP molecule and produce $pppA_3$. Subsequent polymerization terminated by cyclization results in cA_3 to cA_6. (**E**) HPLC-MS analysis and reaction scheme of StCsm-mediated conversion of synthetic linear OA triphosphates into the corresponding cOAs. $(M-H)^-$ and $(M-2H)^{-2}$ denote ion mass/charge ratio values for different ionization forms. Mw_{theor} denotes the predicted molecular mass in daltons.

Downloaded from https://www.science.org at Shanghai Normal University on March 29, 2025

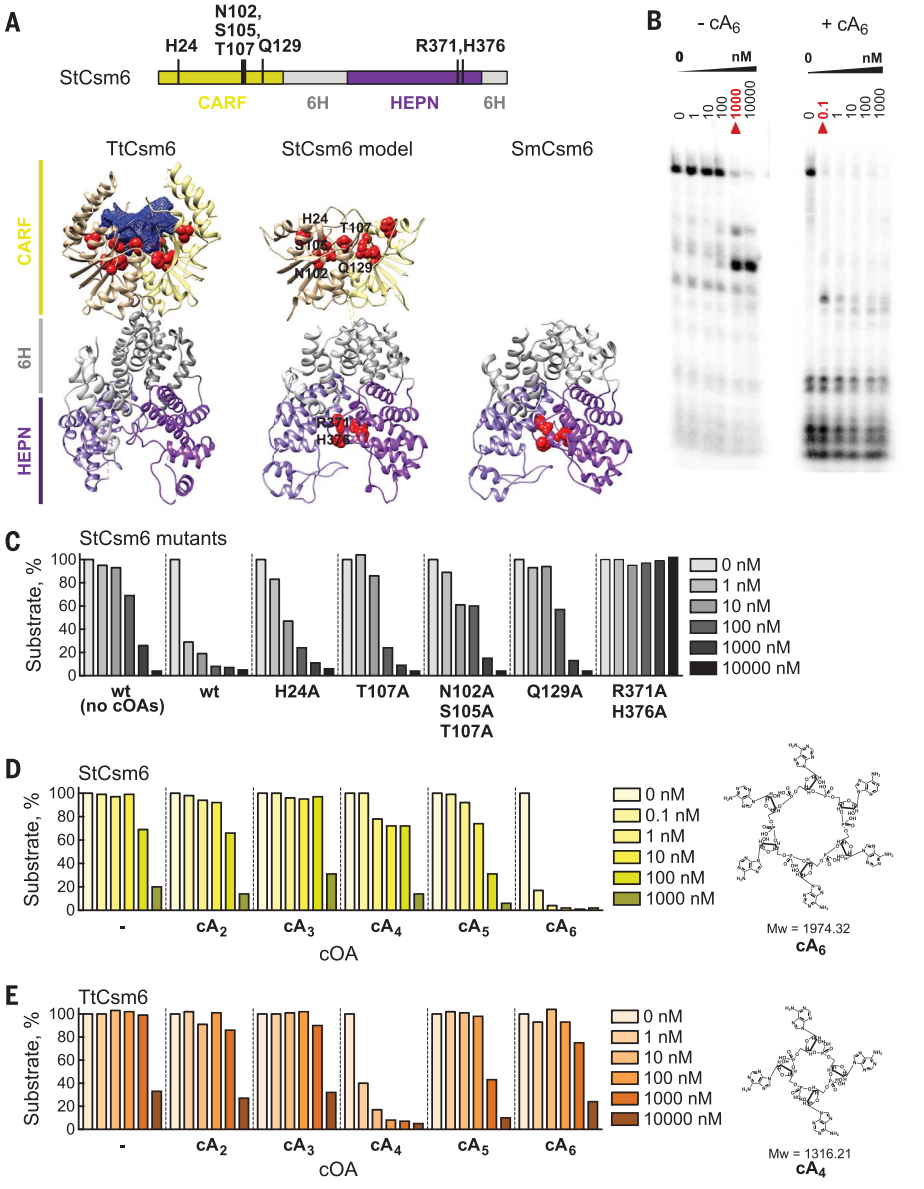


Fig. 3. Csm6 ribonuclease activation by StCsm-produced cOAs. (**A**) Domain arrangement of StCsm6. Conserved residues subjected to alanine mutagenesis are indicated above the colored boxes and as red spheres in the ribbon structures below. Blue mesh denotes the putative ligand binding cleft. (**B**) StCsm6-mediated ssRNA cleavage in the absence and presence of 0.5 nM cA_6. Red indicates the StCsm6 concentration that is required for efficient ssRNA hydrolysis. (**C**) RNase activity of StCsm6 mutants. (**D**) Dependence of StCsm6 RNase activity on nucleotide effectors. (**E**) Dependence of TtCsm6 RNase activity on nucleotide effectors. Chemical structures of cA_4 and cA_6 are shown on the right.

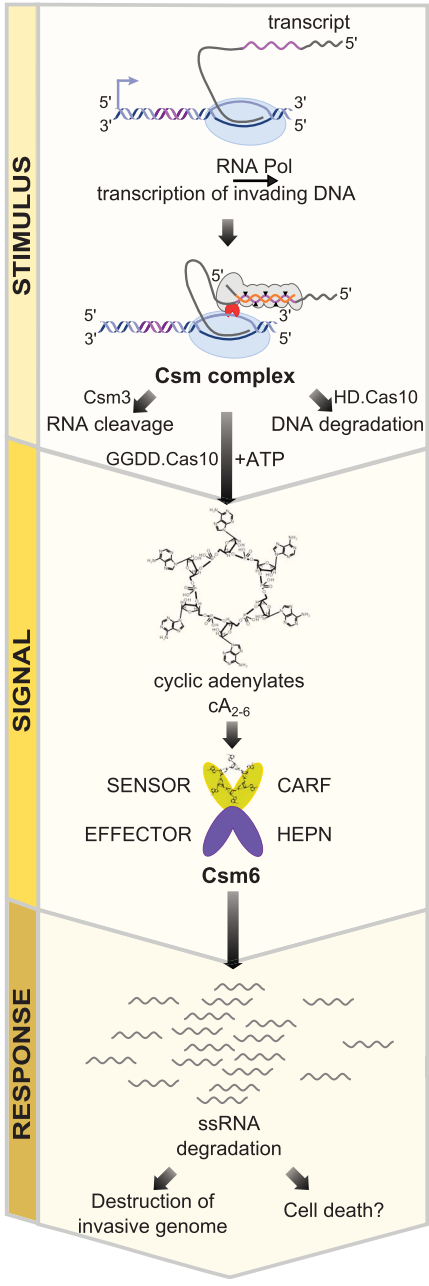


Fig. 4. Mechanism of signaling in type III CRISPR-Cas systems. A transcript from an invading DNA serves as a stimulus for the StCsm complex (RNA Pol, RNA polymerase). Recognition of the invasive transcript by the Csm complex through base-pairing between the crRNA and the transcript promotes the three activities of Csm: (i) Csm3-mediated cleavage of the transcript itself, (ii) degradation of the corresponding invading DNA by the HD domain of Cas10, and (iii) synthesis of cOAs by the Palm domain of Cas10. The resultant cOA is a signaling molecule that is recognized by the sensory CARF domain in Csm6, which in turn activates the effector HEPN domain of Csm6. Thus, activated Csm6 effectively degrades ssRNA, which could buy the time necessary to ensure the destruction of the invasive genome or eventually lead to cell death.

superkingdoms of life as intracellular messengers conveying specific and global signals (*14*). They are synthesized in a cell by specific enzymes in response to different stimuli and are recognized by sensor domains embedded within different effector proteins. Linear 2′,5′-OAs (n = 3 to 30) as signaling molecules have been identified in vertebrates, where they are synthesized in response to sensing of double-stranded viral RNA, leading to stimulation of latent HEPN ribonucleases to destroy invading RNA (*27*). However, in prokaryotes, signaling systems centered on cyclic oligonucleotides (n > 2) have remained unknown until now. Thus, our data reveal a cOA-based signaling pathway in prokaryotic defense systems. We show that cOAs, synthesized by the StCsm effector complex in response to the binding of target RNA, act as second messengers that activate nonspecific RNA degradation by the dormant Csm6 ribonuclease through binding to the sensory CARF domain (Fig. 4). This signaling pathway could serve as a contingency plan in case the coordinated degradation of transcriptionally active DNA and its transcripts by the Csm effector complex fails to combat the virus. It remains to be established whether cOAs could also act as extracellular messengers

Downloaded from https://www.science.org at Shanghai Normal University on March 29, 2025

that enable bacterial communication. Interestingly, some CARF-domain proteins are not associated with type III CRISPR-Cas systems, raising a question of how the cOA signaling molecule is generated in these cases (*18*). As described here, signaling pathways involving cOAs (i) provide an additional level of control for the antiviral defense system (*21*), potentially inducing dormancy to buy time for the host to destroy the invader or promote programmed cell death of the host (*28*); (ii) ensure a mechanism for signal amplification; and (iii) allow robust discrimination from other signaling pathways in the cell.

REFERENCES AND NOTES

1. G. Tamulaitis, Č. Venclovas, V. Siksnys, *Trends Microbiol.* **25**, 49–61 (2017).
2. M. A. Estrella, F. T. Kuo, S. Bailey, *Genes Dev.* **30**, 460–470 (2016).
3. M. Kazlauskiene, G. Tamulaitis, G. Kostiuk, Č. Venclovas, V. Siksnys, *Mol. Cell* **62**, 295–306 (2016).
4. T. Y. Liu, A. T. Iavarone, J. A. Doudna, *PLOS ONE* **12**, e0170552 (2017).
5. A. I. Cocozaki *et al*., *Structure* **20**, 545–553 (2012).
6. K. S. Makarova, L. Aravind, Y. I. Wolf, E. V. Koonin, *Biol. Direct* **6**, 38 (2011).
7. X. Zhu, K. Ye, *FEBS Lett.* **586**, 939–945 (2012).
8. A. M. Burroughs, D. Zhang, D. E. Schäffer, L. M. Iyer, L. Aravind, *Nucleic Acids Res.* **43**, 10633–10654 (2015).
9. J. R. Elmore *et al*., *Genes Dev.* **30**, 447–459 (2016).
10. P. Samai *et al*., *Cell* **161**, 1164–1174 (2015).
11. T. Osawa, H. Inanaga, T. Numata, *J. Mol. Biol.* **425**, 3811–3823 (2013).
12. A. Schmidt *et al*., *Proc. Natl. Acad. Sci. U.S.A.* **76**, 4788–4792 (1979).
13. M. Fujimoto, A. Kuninaka, H. Yoshino, *Agric. Biol. Chem.* **38**, 1555–1561 (1974).
14. C. Opoku-Temeng, J. Zhou, Y. Zheng, J. Su, H. O. Sintim, *Chem. Commun.* **52**, 9327–9342 (2016).
15. K. S. Makarova, Y. I. Wolf, E. V. Koonin, *Biochem. Soc. Trans.* **41**, 1392–1400 (2013).
16. G. Tamulaitis *et al*., *Mol. Cell* **56**, 506–517 (2014).
17. O. Niewoehner, M. Jinek, *RNA* **22**, 318–329 (2016).
18. K. S. Makarova, V. Anantharaman, N. V. Grishin, E. V. Koonin, L. Aravind, *Front. Genet.* **5**, 102 (2014).
19. N. F. Sheppard, C. V. Glover 3rd, R. M. Terns, M. P. Terns, *RNA* **22**, 216–224 (2016).
20. V. Anantharaman, K. S. Makarova, A. M. Burroughs, E. V. Koonin, L. Aravind, *Biol. Direct* **8**, 15 (2013).
21. W. Jiang, P. Samai, L. A. Marraffini, *Cell* **164**, 710–721 (2016).
22. J. Bondy-Denomy *et al*., *Nature* **526**, 136–139 (2015).
23. N. G. Lintner *et al*., *J. Mol. Biol.* **405**, 939–955 (2011).
24. E. Topuzlu, C. M. Lawrence, *RNA Biol.* **13**, 254–257 (2016).
25. X. Yan, W. Guo, Y. A. Yuan, *RNA Biol.* **12**, 749–760 (2015).
26. O. O. Abudayyeh *et al*., *Science* **353**, aaf5573 (2016).
27. R. H. Silverman, *Cytokine Growth Factor Rev.* **18**, 381–388 (2007).
28. E. V. Koonin, F. Zhang, *BioEssays* **39**, e201600186 (2017).

ACKNOWLEDGMENTS

We thank A. Rukšėnaitė and L. Taujenis (Thermofisher Scientific) for help with HPLC-MS experiments; A. Silanskas for HPLC purification of adenylates; P. Moller Martensen (Aarhus University) for a kind gift of pOAS1 and pPDE12 plasmids; P. Horvath (DuPont) for a kind gift of *S. thermophilus* DGCC8004 strain and discussions; and S. E. Halford for critical reading of the manuscript. G.T. acknowledges support from the Research Council of Lithuania (grant APP-3/2016). M.K., G.K., G.T., and V.S. are inventors on patent applications related to the work described in this manuscript: V.S., M.K., and G.T. on international patent application PCT/IB2015/056756 submitted by Vilnius University, which covers the StCsm complex and its use for directed RNA cleavage, and V.S., M.K., G.K., and G.T. on U.S. provisional patent application 62/512868 submitted by Vilnius University, which covers production of cyclic oligoadenylates and their use as allosteric regulators. Expression plasmids used in this work are available from G.T., M.K., or V.S. under a material transfer agreement with Vilnius University.

SUPPLEMENTARY MATERIALS

www.sciencemag.org/content/357/6351/605/suppl/DC1
Materials and Methods
Supplementary Text
Figs. S1 to S24
Table S1
References (*29*–*38*)

8 June 2017; accepted 22 June 2017
Published online 29 June 2017
10.1126/science.aao0100

Downloaded from https://www.science.org at Shanghai Normal University on March 29, 2025